Medical Image Compression with Lossless Regions of Interest

Jacob Ström and Pamela C. Cosman *

August 1, 1996

Number of manuscript pages = 50

Header and information = pages 1-2

Abstracts in English and French = pages 3-4

Text = pages 5-26

References = pages 27-34

Figures = pages 35-48

List of figures = pages 49-50

There are 0 tables.

There are 14 figures.

*J. Ström is a graduate student in the Department of Electrical Engineering, Linkoping University, S-581 83 Linkoping, Sweden. P.C. Cosman is with the Department of Electrical and Computer Engineering, University of California, San Diego, La Jolla, CA 92093–0407. This work was funded by a National Science Foundation Career Award, contract number MIP-9624729, and by the BMDO Focused Research Initiative on *Photonics for Data Fusion Networks*, contract number F49620-95-1-0538.

Key Words:

Region-of-interest compression

Medical image compression

Regionally lossless coding

Radiology information systems

Abstract

Many classes of images contain some spatial regions which are more important than other regions. Compression methods which are capable of delivering higher reconstruction quality for the important parts are attractive in this situation. For medical images, only a small portion of the image might be diagnostically useful, but the cost of a wrong interpretation is high. Algorithms which deliver lossless compression within the regions of interest, and lossy compression elsewhere in the image, might be the key to providing efficient and accurate image coding to the medical community. We present and compare several new algorithms for lossless region-of-interest (ROI) compression. One is based on lossless coding with the S-transform, and two are based on lossy wavelet zerotree coding together with either pixel-domain or transform-domain coding of the regional residual. We survey previous methods for region-based coding of medical images.

Abstract

Un bon nombre d'images contiennent des régions dans l'espace qui sont plus importantes que d'autres. Les méthodes de compression qui sont capables de restituer la meilleure qualité de reconstruction pour ces parties importantes deviennent alors très intéressantes. Dans le cas des images médicales, seulement une seule portion d'image peut être utile pour établir un diagnostic, mais le cout d'une mauvaise interprétation peut être très élevé. Les algorithmes qui effectuent une compression sans perte dans les régions intéressantes et une compression avec pertes partout ailleurs, pourraient être la solution pour fournir un codage d'image efficace et précis pour le domaine médical. Nous présentons et comparons plusieurs algorithmes pour la compression sans perte des régions d'interet (ROI). L'un est basé sur le codage sans perte avec la transformation en S, et deux autres sont basés sur le codage avec pertes (ondelettes "zerotree"); parmi ces 2 derniers, en codant les residus par région, l'un fonctionne dans le

domaine des pixels, l'autre dans le domaine de la transformé par ondelette. Nous balayons rapidement les methodes deja publiées pour le codage basé sur le principe de régions.

1 Introduction

The easy, rapid, and reliable digital transmission and storage of medical and biomedical images would be a tremendous boon to the practice of medicine. Patients in rural areas could have convenient access to second opinions. Patients readmitted to hospitals could have earlier imaging studies instantly available. Rather than waiting for others to finish with hardcopy films, medical and surgical teams collaborating on patient care could have simultaneous access to imaging studies on monitors throughout the hospital. This long-term digital archiving or rapid transmission is prohibitive without the use of image compression to reduce the file sizes. For example, a single analog mammogram might be digitized at 4096 $\times$ 4096 pixels $\times$ 16 bpp. This file would be over 33 megabytes (MB). In lossless compression, the original image is exactly recoverable from the compressed format; with lossy coding, it is not, but vastly greater compression is achieved. However, lossy schemes are viewed with suspicion by many members of the medical and scientific community; image alteration might entail loss of diagnostic or scientific utility. Many physicians feel they cannot trust lossy compression which mostly delivers exquisite quality and yet which can, without warning, introduce medically unacceptable artifacts into the image. After segmenting an image into regions (either automatically or manually) it is possible for a compression algorithm to deliver different levels of reconstruction quality in different spatial regions of the image. One could accurately (losslessly) preserve the features needed for medical diagnosis or for scientific measurement, while achieving high compression overall by allowing degradation in the unimportant regions. Such coding, which we term *regionally lossless coding* or *lossless-ROI coding*, may be the key to having physicians and scientists entrust image data to compression.

In radiology, the discussion of image compression often divides into three separate uses: com-

pression before primary diagnosis (for rapid transmission), compression after primary diagnosis (for long-term archiving), and compression for database browsing (where progressivity would be useful). Compression occurring before primary diagnosis is the most controversial use of lossy compression. However, it might prove useful in cases where the interpreting radiologist is at a remote site and lossless compression cannot be used. For example, the patient's situation might require such rapid action that the time for lossless transmission of original images cannot be countenanced, or the bandwidth for real-time lossless video transmission might not be available. Compression after primary diagnosis might be useful for long-term digital archiving. Here it is easy to imagine how region-based coding might play a role, since the primary interpretation of a film can perhaps be used for providing the region segmentation. A third use of compression is for providing *progressive* transmission capabilities when receiving images over a network. With progressive coding, image quality incrementally improves as more bits arrive. Early versions of an image can be good enough to show that the image is not of interest; transmission can then be 'nipped in the bud.' Progressive codes can be designed to be eventually lossless, so that if the user waits long enough (e.g., 30 seconds) the image will be exactly equal to the original, but over the short term (e.g., 0.5 seconds) the image would already be useful. Region-based methods that take image content into account might deliver a useful version more rapidly.

As an example, Figure 1a shows an MR brain scan with cancerous tumors circled. Following its use in primary diagnosis, this image could be compressed so as to perfectly preserve this region. Allowing graceful degradation in the rest of the image could yield high compression. The original image has a grayscale resolution of 8 bits per pixel (bpp); Figure 1b shows it compressed to 0.08 bpp. This is not of sufficient quality for a physician to measure the effects of a treatment. Figure 1c shows an example in which the compressed image has the circular tumor region at original quality,

and it represents what one might wish to obtain from a regionally lossless scheme. This image is suitable for comparison and still provides dramatically higher compression than can be achieved by schemes which are lossless everywhere. This image could include a circle that makes clear the boundary of the lossless region. In this example, the important region occupies only 4% of the pixels in the image. After the entire image has been compressed by a factor of 100:1, the important region would represent 80% of the total file size if it were not compressed.

2 Background

In region-based coding, the input image is segmented, i.e., divided into spatial regions. A schematic is shown in Figure 2. The regions may differ in their grayscale characteristics or in their importance levels. The division into regions can be useful for two very distinct purposes. Segmentation can allow the use of encoding schemes tailored for the different regions, and it can allow the assignment of different quality levels to the different regions. In the first case, the difference between quality levels Q_1 and Q_2 might be negligible, but the segmentation allows the profitable use of different methods M_1 and M_2. In the second case, the methods might be identical except for their bit allocations, and the goal is to produce different quality levels. It is possible, of course, that the segmentation might be useful for both purposes.

2.1 Regions with different encoding methods

Most work in region-based coding has focused on the former goal – identifying regions with different grayscale characteristics which would profit from the use of different encoding schemes. The earliest work on region-based coding called itself "contour-texture" coding [25, 27]. Region-growing seg-

mentation was followed by approximation of internal areas using 2-D smooth polynomial functions of order 0, 1, or 2. The region-growing was based on gray-level intensity, and a post-processing step merged small regions. In coding, the boundaries were represented by a combination of straight lines, circular arcs, and pieces of original boundaries. Later variations on this theme included using split-and-merge segmentation [26], imposing smooth boundary constraints, allowing internal behavior to be represented by either polynomial approximation or vector quantization [17, 11, 14] and a variety of other ideas. Boundaries can be described in a variety of different ways, including chain codes, polygonal approximations, signatures, and boundary segments [18]. These boundary representations can be losslessly encoded. There is an inherent trade-off between the accuracy of object segmentation and the overhead for coding the description of the segmentation. Segmentation can be very useful for videophone coding, where it is possible to exploit extensive a priori knowledge about the scene (e.g., existence of a face symmetry axis and relative approximate locations of the primary facial features) (see, e.g., [29]).

Several region-based coders have been used in the context of multiresolution decompositions. Baseri and Modestino applied methods of boundary description and parametric polynomial fitting to the baseband of a subband decomposition [1]. In this way, the superior performance of subband coding could be combined with the ability of polynomial functions to model low-frequency regions of natural images. A division of subbands into edge regions (found separately in each subband), texture regions (in common for all subbands), and low-activity regions was proposed in [28]. Good results were obtained by extracting arbitrarily shaped regions in each band, and using different quantizers and different bit allocations for each class of sub-region in each band.

2.1.1 Regions for motion compensation

Region-based methods have been finding particularly fruitful applications in the compression of motion sequences (see, e.g., [51, 31, 15, 30, 33, 54, 32, 16, 4, 49, 10, 55, 19, 20, 43]). These methods are often called "object-oriented" compression techniques, since a moving region is often a discrete object. Object-oriented approaches are generally aimed at very low bit rate video coding. Typically, object-oriented coding algorithms segment each image into regions of uniform motion and estimate motion of these regions to generate more accurate motion compensated images. Compared with block-based motion compensation, object-oriented motion compensation requires extra computation to perform the segmentation, extra bits to encode the boundary information (which is often encoded by a chain code), but fewer bits to encode the motion-compensated prediction error. Another slightly different approach is to use a simple block-based motion estimator, and then to use an object-oriented approach to segmenting the motion-compensated difference frame. The difference image can, for example, be segmented into regions of high and low activity, and the low activity regions can be left unencoded.

2.2 Regions with different quality levels

A smaller number of studies on region-based coding have focused on the second goal – providing different levels of quality in different spatial regions of an image. In [40], aerial images were segmented into non-homogeneous regions (e.g., roads, buildings) which were considered important, and textured homogeneous regions (e.g., agricultural or undeveloped areas) which were less important. The quality goals were to achieve "information preservation" for the important parts, and "image realism" for the remainder. Texture modeling was performed in the wavelet domain within

polygonal regions that were defined by their relatively homogeneous statistics in the image domain. In the non-homogeneous regions, the subband data was adaptively scalar quantized. The quantized coefficients, texture parameters, and region geometries were then losslessly encoded. In this example, both different quality levels and different encoding methods resulted from the segmentation. A similar goal appeared in [22], in which images were segmented and coded with polynomial approximations. Such schemes can be very inefficient for textured regions, since they tend to get approximated with a large number of uniform regions. A pre-processing step was used to identify textured regions and reduce the number of regions there. Cheng and Kuo used a JPEG-like scheme in which different quantization tables were used for different regions [9]. In this work, the block discrete cosine transform (DCT) was replaced with a fully decomposed wavelet transform. Coefficients from different bands were grouped into blocks, and JPEG-style quantization and entropy coding were then applied. A user selects a rectangular region of interest, and blocks in this region are subjected to a less coarse quantization. For a video application, the system tracks the position of the region of interest. Bedini, et al, focus on videotelephone sequences in which the speaker's head is detected using active snakes [2]. Internal facial features such as the eyes and the mouth are subsequently detected and coded more accurately. Similar goals for videotelephone sequences are discussed in [5].

2.2.1 Quality levels for medical images

Several studies have focused on different region-based quality levels for medical applications [35, 36, 37, 53, 52, 34, 24, 6, 7]. The general theme is that diagnostically important regions must be preserved at high quality, whereas the rest of the image is only important in a contextual sense, helping the viewer to observe the position of the ROI within the original image. The proposed

schemes differ according to the segmentation methods (manual vs. automatic) and segmentation goals (a background/foreground distinction or a more focused segmentation), and according to the compression methods (DCT, vector quantization, wavelets, etc.) and compression goals (lossless ROI vs. lossy ROI).

In [35], MR brain images were segmented, and different segments were encoded with vector quantizers at different rates. In this work, region boundaries were not explicitly coded; the members of this class of images were assumed to have sufficient spatial stationarity that the region locations could be assumed to match the standard. The algorithm was not robust against the situation where an individual scan had the brain portion significantly displaced with respect to the average for the class. In later work, this problem was fixed and yet encoding of region boundaries was still avoided by basing the segmentation on the small, low resolution version of the image which was transmitted first [36]. The lowest band (LL_4) of a 4-level wavelet decomposition was automatically segmented into 3 regions of differing diagnostic importance. Based on this segmentation, bits and quality were allocated to the corresponding regions of the next subbands (LH_4, HL_4, HH_4). These four encoded and reconstructed bands could then undergo a single round of inverse transforming to produce a new baseband (LL_3). In its turn, this baseband could be segmented and bits could be assigned to the other bands. With a recursive application of inverse transforming and segmenting, occurring at both the encoder and decoder, the bit allocation could be tracked through all the bands. The structure is shown in Figure 3. Another method that involved an automatic segmentation into 3 regions was [34], in which ventricular cineangiograms were compressed by forming differences within each region, and approximating those residuals with smooth functions.

A region-based method using predictive pruned tree-structured vector quantization was reported in [37]. Here, simple methods based on thresholding, connectivity, and boundary smoothing were

used to segment CT chest scans into foreground and background. The boundary was encoded with a chain code. The background was not encoded, and was displayed as black by the decoder. The paper showed that the segmentation improved performance not only because no bits would be wasted on the background, but also because a more accurate predictor could be designed by using only the foreground regions of the training set. Another method focusing on foreground/background segmentation was [53] which exploited the fact that a large proportion of a mammogram consists of uninteresting background. A self-organizing neural network was first used to separate the breast area from the background. Then an optimized JPEG coding algorithm was used to code the segmented breast area only, at near lossless quality.

In [52], a ROI-DCT algorithm was proposed, in which an 8×8 block DCT is performed on an image, and more DCT coefficients are retained for blocks inside the ROI, so that the ROI ends up with high quality. While not precisely segmentation-based methods, in [6, 7], methods for adaptively quantizing wavelet coefficients were developed with an eye towards preserving strong edges. The goal is to accurately preserve structures and boundaries which might be subjected to quantitative measurements by a radiologist.

The studies described so far have been concerned with segmentation-based *lossy* coding of medical images, where the ROI gets higher, but not lossless, quality. A small number of previous studies have also focused on segmentation-based *lossless* coding of medical images, in which all regions retain lossless quality, but different lossless encoding methods might be used for different regions such as background and foreground (see [45, 47]). One previous study focused on lossless-ROI coding for medical images, in which the ROI is lossless but the remainder of the image sustains degradation [24]. This study compared three different methods: a DCT method, a DCT/HINT method and a HINT method. The DCT-based method was found to be the best among the three in terms

of compression ratio, algorithmic complexity, and quality of reconstructed image. First the entire image was transformed, quantized and encoded using 8×8 block DCTs, a scalar quantizer and Lempel-Ziv (LZ) coding. Then the image was reconstructed and a residual image was computed. The residuals of the pixels inside the ROI region were coded using LZ coding. This method is close to that described in [50], in which JPEG followed by adaptive prediction and adaptive arithmetic coding of the residual were used to encode an image losslessly in its entirety. A lossless-ROI scheme employing a version of pyramid coding (adapted MIP texture mapping) was described in [12] in the context of gaze-contingent displays, but specific compression results were not included.

2.3 Multiresolution decompositions

The goal of our work is to develop and compare algorithms which deliver different levels of reconstruction quality in different portions of the image, specifically where the region-of-interest R has no loss (perfect reconstruction). We focused on multiresolution coding methods such as wavelet zerotree coding [44] and the S-transform [39, 21, 38], since multiresolution methods are currently the basis for the best general-purpose lossy and lossless compression of still images (e.g., [44, 42, 41, 13]).

The basic concept of wavelet zerotrees is as follows. A subband decomposition is produced by an analysis filter bank followed by downsampling. Any or all of the resulting subbands can be further input to an analysis filter bank and downsampling operation, for as many stages as desired. In a two-channel separable system, the initial high-pass and low-pass filters and downsampling are applied to the rows of an image. The subsequent filters and downsampling are then applied to the resulting columns. The image is split into four bands, denoted LL_1, LH_1, HL_1, and HH_1, according to whether the rows and columns received the low-frequency or high-frequency filtering.

The reconstruction operation consists of an upsampling operator followed by a synthesis filter bank. If only the low band LL_1 is further decomposed, this is referred to as an octave-band decomposition. In an octave-band decomposition, each coefficient X_i (except those in the lowest band and the three highest bands) is related to exactly four coefficients in the next higher band. Those four coefficients correspond to the same orientation and spatial location as X_i does in the original image. Each of these four is in turn related to four in the next band, and so on. These coefficients are collectively called the *descendants* of X_i. The relationship is depicted in Figure 4. In an octave-band decomposition, it is often true of image data that when a coefficient X_i has magnitude less than some threshold T, all of its descendants will also. The collection of coefficients is then called a *zerotree* with respect to the threshold T, and the coefficient X_i is called the *zerotree root*. Shapiro's embedded zerotree wavelet (EZW) algorithm uses this zerotree structure to efficiently "divide and conquer" the coefficients in an iterative SQ approach. The zerotree root is the wavelet equivalent of the end of block (EOB) symbol in JPEG coding. That is, when a sequence of scanned coefficients ends with a tail of zeros, one simply cuts off the tail with a special symbol. The zerotree grows exponentially with the depth, while in JPEG, there is no such growth, thus making the zerotree potentially more powerful.

A hierarchical subband decomposition must satisfy two conditions in order to allow lossless compression. The filter bank must have the property of perfect reconstruction. This is not the case for standard QMF filters, which are called near-perfect-reconstruction (near-PR) filters [23]. Secondly, it must be possible to represent the subband coefficients with a limited number of bits. These considerations lead to a constrained choice of filters. Egger and Kunt designed a lossless zerotree scheme based on a morphological subband decomposition, in which the coefficients of the subbands are signed integers, requiring 9 bits for their representation [13]. Said and Pearlman

designed a lossless zerotree scheme using what they called the S+P transform [42] a simple pyramid multiresolution scheme (the S-transform) which was enhanced via predictive coding.

The S transform allows perfect reconstruction, and has been used for lossless medical image compression [39, 21]. The one dimensional S-transform maps a sequence of integers $c[n], n = 0, \ldots, N-1$ into two sequences $l[n]$ and $h[n]$ of half the length:

$$l[n] = \lfloor (c[2n] + c[2n+1])/2 \rfloor, n = 0, \ldots, N/2 - 1$$

$$h[n] = c[2n] - c[2n+1], n = 0, \ldots, N/2 - 1$$

where $\lfloor \cdot \rfloor$ denotes downward truncation. The transform is similar to the wavelet Haar transform. The two dimensional S-transform is performed by taking the one dimensional transform first on the rows, and then on the columns. The variation of the S-transform presented in [42, 41], called the S+P transform, uses prediction to further lower first order entropy and improve the overall compression performance.

3 Methods

3.1 Segmentation

In this work, the regions of interest were selected by hand. For a real application, a number of possible scenarios can be envisioned. It is very common for radiologists today, looking at hardcopy diagnostic films, to make quick circles with a grease pencil around the things they find noteworthy in the image. Often the written or dictated report of the radiologist makes reference to something which was marked on the film. Radiologists cannot reasonably be asked to "Mark the region which should get lossless compression." However, they could perhaps be encouraged to "circle something

if it is important," especially if they were going to make some kind of mark anyway, as a reference point for their report. So, at the time of primary interpretation of the film, location of the ROI might be relatively easily obtainable. The information could then be used to compress it for long-term storage. However, it is reasonable to assume that greatest clinical utility would come only from a reliable automatic segmentation system. We may not be far off from a time when computer segmentation could locate a sensible region-of-interest in many images. The system would not have to be correct all the time in order to be useful. We can imagine, for example, that radiologic archiving systems might evolve into some kind of two-tiered structure. One tier will provide for long-term image accessibility, in which all original images are available with some delay. The second tier will have digital images available immediately, but only by employing heavy compression. Even if the automatic segmentation system only targets the correct ROI 80% of the time, in this two-tiered archive, lossless-ROI coding might be very useful. In 80% of cases the fast tier service would rapidly and conveniently provide the diagnostician with the accurate and confident information of the correctly-located lossless-ROI image. In the other 20% of cases, the original image could be retrieved after some delay. In either situation, the initial interpretation would be performed on the original image, and the coding would be used afterwards for long-term storage. So viewing of the coded lossless-ROI image might only occur in the context of an already-diagnosed patient who is being seen for later comparison. In this situation the radiologist could be assumed to know, upon viewing the coded image, whether the displayed ROI was in the right place, or whether retrieval of the original was called for. The validity of this assumption could be tested by simulating the use of the ROI selection and encoding process in a clinical experiment.

3.2 Encoding

There are two basic approaches to providing a lossless region-of-interest using a multiresolution decomposition:

1. Use a decomposition that permits perfect reconstruction. Quantize the coefficients for the entire image, to attain the desired bit rate or quality constraint for the background region $\bar{R}$. Then, refine the quantization to the point of perfect reconstruction only for coefficients that impact on region R.

2. Use a decomposition that does not necessarily permit perfect reconstruction. Quantize the coefficients for the entire image, to attain the desired bit rate or quality constraint for the background region $\bar{R}$. At this point, let $\hat{R}$ denote the lossy recontruction of R (see Figure 5).

   We now have the option of computing and losslessly encoding the *regional difference image*. This image contains zero values in the region $\bar{R}$, and contains the difference between R and $\hat{R}$ in the region R. Alternatively, once the desired bit rate or quality constraint has been met for the background region $\bar{R}$, we could continue for a while with refining the lossy representation of the important region R, and then switch to lossless encoding of the regional difference image. In other words, once $\hat{R}$ is achieved, a lossless representation for R can be reached by apportioning different amounts of the work between the lossy algorithm used at the start and the lossless algorithm to be used at the end.

   There are two basic ways in which the regional difference image can be losslessly compressed:

   - A pixel-domain lossless method, such as adaptive arithmetic coding or Lempel-Ziv coding, can be applied to the pixels inside the region R.

- A transform-domain method might not be adaptable to the arbitrary shape of R, and might have to include some or all of the (zero-valued) pixels outside. A variety of methods have been recently introduced for transform coding of arbitrarily shaped regions (see, e.g., [8, 46, 3, 48]) but the focus has been mainly on lossy techniques.

In both cases, the decoder must either infer the location of the lossless region, or must be explicitly told the boundaries of the region. If the decoder is explicitly told, those bits must be included in the final rate. In our work, we ignore the issue of region description, assuming that the lossless region will be composed of a small number of circles or rectangles that can be explicitly described with a negligible number of bits. For example, for a rectangle, the encoder could transmit the coordinates for one corner, and the height and width in pixels. For an image of size 512×512, this would entail at most 36 bits. Similarly, for a circle, one could transmit the coordinates of the center, and the radius.

In the following, we present lossless ROI coding using each of the two basic approaches outlined above. For the case where a lossy algorithm is used initially, necessitating a switch to a lossless algorithm, we examine various possible divisions of effort between the coding stages.

3.3 The S-algorithm

The first approach is to decompose the image using a method which allows perfect reconstruction. For this we chose the S-transform together with the zerotree-style successive refinement of coefficient values. Let R_{Tr} denote all the coefficients in the transform domain that will have an impact on R after the inverse transform. The idea of the S-algorithm is to successively refine all coefficients until a certain bit budget B is exhausted. After this, only the coefficients in R_{Tr} are refined, until they

are losslessly described. Figure 6 shows a flowchart of the algorithm.

While the lossless S+P transform of [42] outperforms the S-transform, the added element of prediction makes each coefficient dependent upon the previous one. An error in a coefficient that was outside R_{Tr} (for the S-transform) can now propagate to a coefficient inside. Thus all coefficients in the decomposition must be lossless (which is not our goal) or else appropriate initial prediction conditions must be supplied for the arbitrarily shaped region. When decompressing, all the coefficients that affect R will be correct, and R will thus be losslessly recovered. A disadvantage of the S-transform is that it introduces block artifacts in the lossy parts (see Figure 7), due to the short support of the S "filters".

3.4 The WA-algorithm

A second approach is to choose a filter that does a better job of decorrelating pixels but that does not provide perfect reconstruction, and then to make up the difference by lossless pixel-domain coding. Coefficients for the entire image are successively approximated until the desired target bit rate is met. Then the coefficients in R_{Tr} are further refined until all the (inverse transformed) pixels in R differ from the original image pixels by an amount less than d. Lastly, arithmetic coding is performed in the pixel domain on the residual for the R region. By changing d, one adjusts the workload between the wavelet zerotree encoder and the arithmetic encoder. We call this combined wavelet and arithmetic algorithm the WA-algorithm. Its flow graph is shown in Figure 8.

The wavelet zerotree encoder will generally perform better with longer filters to decorrelate the pixels. Then the number of coefficients affecting each pixel is greater, and thus R_{Tr} grows. The fraction of the subband contained in R_{Tr} grows as we go to lower resolution subbands. We will

thus have a good representation of the higher frequencies only in R and immediately outside, while the lower frequencies will still be accurate a little further away from R. As shown in Figure 9, this produces a graceful degradation in quality as we move away from R.

One might think that a bigger R_{Tr} must imply a waste of bits and therefore worse rate/distortion performance. This need not be the case. If the encoding of R also improves the quality of the background $\bar{R}$, we do not need so many bits to describe the background in the first place, and we could terminate the first encoding step earlier. This would correspond to stealing bits from the more remote parts of the background, at the expense of the nearer parts. The uneven distribution of quality would not be properly reflected in the average PSNR score of the background.

3.5 The WS+P algorithm

The third approach begins as the second one does, with a lossy embedded wavelet zerotree coder, and then uses the lossless S+P transform to make up the difference as needed for R. The wavelet zerotree method provides a lossy representation of the image. This is then subtracted from the original to provide the regional difference image. As shown in Figure 5, the regional difference image is set to zero everywhere outside R. Since the residual is to be encoded losslessly, modulo 256 arithmetic can be used, so that the residual image can be represented in 8 bits. A constant value of 128 (modulo 256) is added to all coefficients. This has the advantage of encoding residuals of similar magnitudes with bytes of similar values. For instance, the residual sequence $-1, 1, -1, 1$ is encoded with $127, 129, 127, 129$ instead of $255, 1, 255, 1$ which would yield large high frequency components in the transform. The residual is then transformed with the S+P transform. The coefficients are encoded with a zerotree successive approximation method. Since the image will be

of constant intensity (128) outside R, the prediction quickly goes to zero. Thus the set of nonzero coefficients in the S+P transform domain is not much bigger than the set of R_{Tr} pixels gotten from an S-transform. The smallest set R_{Tr} is found that completely covers the non-zero coefficients. A few bits are used to described this set to the decoder, and the set is used to discriminate among the coefficients when encoding the zerotrees. The algorithm is referred to as the WS+P algorithm, and is described in the flow graph in Figure 10.

4 Experimental results

The three algorithms were implemented by modifying the publicly available C code used in [42, 41] to incorporate the various distinct methods for handling the ROI. The algorithms were tested on a variety of different images: magnetic resonance (MR) brain scans, MR chest scans, computerized tomographic (CT) chest scans, and mammograms. All images were 8-bit grayscale (the CT and mammographic images had their amplitude values linearly rescaled down to the 8-bit dynamic range). Image sizes ranged from 256×256 up to 1500×2000. In each case, a single square ROI was selected. In the case of images displaying pathology, the ROI focused on a region of primary diagnostic importance. In the case of normal images, the ROI was located near the center of the image. Different sizes of the ROI region were examined, ranging from only a few pixels on a side up to approximately 60% of the total area of the image. The methods were compared with different fixed values of (average) background PSNR. In addition, the DCT/LZ method of [24] was implemented for comparison. (Our implementation accomplished the LZ coding using UNIX gzip version 1.2.4, which may not be identical to their algorithm, since the exact version of LZ coding was not stated in [24]). We also implemented a Wavelet-LZ algorithm (W/LZ) similar to the DCT/LZ

but with the wavelet algorithm from [41] instead of the DCT to provide the lossy image. For each ROI size, the file size in bytes was measured for all five algorithms.

The results for the various algorithms were dependent on the selected background PSNR and the size of the ROI. For example, for an average background PSNR of 40 dB, results are shown for various ROI sizes in Figure 11 for a 512×512 CT scan. Note that the WA-algorithm (dotted line) performs well for small ROI sizes. When the ROI is small, the spillover of quality from the ROI is small and the good decorrelation effect of the WA algorithm pays off. For large ROI sizes, it becomes less competitive. The DCT/LZ algorithm (denoted by + symbols) does poorly for all ROI sizes. The S-algorithm (solid line) is not very efficient for small regions but for very large regions it does well. The W/LZ algorithm (dashed line) is the best for the smallest ROIs, but loses to the WS+P algorithm (crosses) for sidelengths bigger than approximately 30 pixels. The WS+P method performs well throughout the range of sizes. These trends were similar for other images tested, although the exact crossing points varied. For example, for a 512×512 section of a mammogram, the W/LZ algorithm was competitive with the WS+P algorithm up to a ROI side length of about 80 pixels, and the WS+P algorithm was superior for larger ROIs.

The WA-algorithm includes an additional adjustable parameter d. After the entire set of coefficients has been described to some desired (low) bit rate, there remains the refinement of the ROI to lossless accuracy. The adjustable parameter controls the allocation of this refinement work between the lossy zerotree coder and the lossless arithmetic coder. A range of possibilities is shown in Figure 12. In this example, the wavelet zerotree coder uses 0.013 bpp initially to produce a constant PSNR of 36 dB for the entire test image (a section of a mammogram). The WA-algorithm can use a variable number of extra zerotree bits for R, so that the maximum absolute error in the ROI is less than d. The x-axis shows the maximum absolute error for the pixels in the ROI at

the point when the coder switches from the wavelet-zerotree description to the arithmetic coder in the pixel domain. The dotted line is the number of extra kbytes used for describing the wavelet coefficients of region R. The dashed line represents the output from the arithmetic coding of the residual. The dot-dashed line is the total number of kbytes to describe the entire image (the two first lines + the constant amount used initially by the wavelet zerotree coder). So, in this case, the overall performance improves as the encoder shifts more work to the arithmetic coder.

This is not always the case. In Figure 13, the role of the arithmetic coder is examined at different background PSNRs for a CT scan. For all 4 curves, the ROI was of fixed size 200×200 pixels. Each curve represents a different background PSNR value (which is also the initial PSNR of the ROI): 28 dB (solid), 32 dB (dotted), 36 dB (dashed) and 40 dB (dash-dot). The y-axis shows file size in kbytes, and the x-axis shows maximum absolute error in the ROI at the point where the arithmetic coder takes over from the zerotree coder. High values of background PSNR make it profitable to let the arithmetic coder do as much work as possible. That is, the ROI is initially encoded by the zerotree encoder to the same high PSNR as the background gets, and all further refinement of the ROI should be done by the arithmetic encoder. For lower values of background PSNR, however, continuing the refinement of the ROI in the wavelet domain past that background PSNR level is a useful way to expend bits up to a point, and we get a minimum on the curve.

Different shapes for the ROI region were also tried briefly. As expected, the WS+P algorithm gives best performance on square ROIs. Other shapes penalize the performance but do not affect the trend; when comparing the WS+P algorithm to the WLZ algorithm, for instance, the WS+P algorithm was still superior if the ROI area was increased sufficiently. For example, a square with a side length of 60 pixels was enough for the WS+P algorithm to be superior to the other algorithm. A circular ROI had to have the same area as an 80 pixel wide square in order for the WS+P

algorithm to be superior. Less compact shapes were also tried, with similar results.

Pictorial examples of the results are given in Figure 14. Figure 14(a) shows an original CT chest scan, of size 512×512, rescaled to 8 bpp grayscale. The white outline of a square ROI is displayed superimposed on the image. Figure 14(b) shows the image compressed to 3953 bytes (0.12 bpp) using the lossy wavelet zerotree method [41] without consideration of the ROI region. Figure 14(c) shows the image compressed to 3953 bytes using the WS+P algorithm to ensure a lossless ROI. The bits required to make the ROI lossless have required a considerable degradation in the rest of the image. Figure 14(d) and (e) are zooms of Figures 14(b) and (c), respectively, showing how the ROI compares for the lossy and lossless cases. For a situation where the radiologist intended to make a detailed measurement of a feature in this area, or a quantitative comparison to another scan, the lossless ROI would be preferable. Of course, with an additional expenditure of bits, one can have both lossless quality in the ROI and high quality in the remainder of the image (see Figure 14(f), at 0.22 bpp).

5 Conclusions

There are quite a few applications in which one would like certain portions of an image to be encoded with higher quality than other portions (e.g., videotelephone sequences where one would like better quality for the face, aerial or satellite images in which some portions are useless due to cloud obscuration, or are less important because they depict uninhabited territory, etc.) Medical images and some scientific images are among the few where people argue that higher quality should actually mean lossless quality. (Indeed, many physicians and scientists have argued that medical and scientific images must always be compressed losslessly everywhere.) However, we propose

that regionally lossless compression methods have the potential for widespread medical acceptance, since they are responsive to the nature of medical images (spatially varying importance levels and statistical characteristics) and to the needs of the radiologist (guaranteed accuracy for diagnostically important regions, no ambiguity about what portions are reliable).

In this paper, we have investigated several possible methods for providing lossless-ROI coding. With the goal of truly lossless coding of a region, quite different techniques are needed compared with the goal of providing higher (but still lossy) quality. Powerful methods for lossy coding may perhaps be applicable only in conjunction with a lossless coder for the regional residual image. We found that the results depended on several factors, including the size and shape of the ROI, and the desired background PSNR. For almost all background PSNRs and larger ROI sizes of interest, a wavelet zerotree coder followed by lossless encoding of the residual with an S+P transform (the WS+P method) gave the best results. For very small ROIs or very high values of background PSNR, simpler methods using wavelet zerotree coding followed by arithmetic or Lempel-Ziv coding became competitive with the wavelet/S+P method. For these simpler methods, the optimal division of the encoding work between the initial wavelet coder and the final entropy coder was found to depend on the background PSNR chosen. These results makes sense. For very small ROIs or for very high values of background PSNR (which is the initial PSNR of the ROI) the residual ROI has very little structure remaining for the S+P transform to exploit. In these situations, simple entropy coding of the residual is a good solution.

Quality evaluation for this type of coding is challenging. While methods can be compared with a fixed (average) background PSNR, methods that provide different quality gradations in the background are not strictly comparable. Diagnostic accuracy simulation studies can be undertaken to determine whether images archived with lossless-ROI coding are as useful as archived original

images when a patient returns to a hospital for a new imaging study, and a diagnostic comparison with the earlier archived image is required. It would also be of interest to see what percentage of the time the chosen ROI corresponds to what the later interpreting radiologist needs to look at during the comparison. There will of course be cases when the ROI does not correspond to what the radiologist needs for comparison, for either manually selected or automatically segmented ROIs.

Continuations of this project might include comparisons of methods for multiple ROI regions, clinical simulations of the encoding methods in a radiological archiving system, and encoding ROI regions of arbitrary shapes. For arbitrary shapes, the actual ROI boundary description may become significant in the total bit count. The requirement for lossless coding in the ROI will have to be factored in to the rate/distortion trade-off between the accuracy of the boundary description and the overhead required for it.

References

[1] R. Baseri and J.W. Modestino. Region-based coding of images using a spline model. In *Proceedings ICIP-94*, volume III, pages 866–870, Austin, Texas, November 1994. IEEE, IEEE Computer Society Press.

[2] G. Bedini, L. Favalli, A. Marazzi, A. Mecocci, and C. Zanardi. Intelligent image interpretation for high-compression high-quality sequence coding. *European Transactions on Telecommunications*, 6(3):255–65, May-June 1995.

[3] M. Bi, S.H. Ong, and Y.H. Ang. Coefficient grouping method for shape-adaptive DCT. *Electronics Letters*, 32(3):201–2, Feb. 1996.

[4] L. Bonnaud, C. Labit, and J. Konrad. Interpolative coding of image sequences using temporal linking of motion-based segmentation. In *Proceedings ICASSP-95*, volume 4, pages 2265–8, Detroit, MI, May 1995. IEEE.

[5] C. Braccini, A. Grattarola, F. Lavagetto, and S. Zappatore. VQ coding for videotelephone applications adopting knowledge-based techniques: Implementations on parallel architectures. *European Trans. Telecomm.*, 3(2):137–144, Mar.-Apr. 1992.

[6] C.W. Chen, Y.Q. Zhang, J. Luo, and K.J. Parker. Medical image compression with structure-preserving adaptive quantization. In *Visual Communications and Image Processing '95*, volume 2501(2), pages 983–94, Taipei, Taiwan, May 1995. SPIE.

[7] C.W. Chen, Y.Q. Zhang, and K.J. Parker. Subband analysis and synthesis of volumetric medical images using wavelet. In *Visual Communications and Image Processing '94*, volume 2308(3), pages 1544–55, Chicago, IL, Sept. 1994. SPIE.

[8] H.H. Chen, M.R. Civanlar, and B.G. Haskell. A block transform coder for arbitrarily shaped image segments. In *Proceedings ICIP-94*, volume I, pages 85–89, Austin, Texas, November 1994. IEEE, IEEE Computer Society Press.

[9] P.Y. Cheng and C.J. Kuo. Feature-preserving wavelet scheme for low bit rate coding. In *Digital Video Compression: Algorithms and Technologies 1995*, volume 2419, pages 385–396, San Jose, CA, Feb. 1995. SPIE.

[10] J.G. Choi, S.W. Lee, and S.D. Kim. Segmentation and motion estimation of moving objects for object-oriented analysis-synthesis coding. In *Proceedings ICASSP-95*, volume 4, pages 2431–4, Detroit, MI, May 1995. IEEE.

[11] F.G.B. De Natale, G.S. Desoli, D.D. Giusto, and G. Vernazza. Polynomial approximation and vector quantization: a region-based integration. *IEEE Trans. Comm.*, 43(2–4, pt.1):198–206, Feb.–April 1995.

[12] A. Duchowski and B.H. McCormick. Simple multiresolution approach for representing multiple regions of interest (ROIs). In *Visual Communications and Image Processing '95*, volume 2501(1), pages 175–86, Taipei, Taiwan, May 1995. SPIE.

[13] O. Egger and M. Kunt. Embedded zerotree based lossless image coding. In *Proceedings ICIP-95*, volume III, pages 616–619, Washington, D.C., October 1995. IEEE, IEEE Computer Society Press.

[14] S. Fioravanti. A region-based approach to image coding. In J.A. Storer and M. Cohn, editors, *Proceedings of the 1994 IEEE Data Compression Conference*, page 515, Snowbird, Utah, 1994. IEEE Computer Society Press.

[15] V. Garcia-Garduno, C. Labit, and L. Bonnaud. Temporal linking of motion-based segmentation for object-oriented image sequence coding. In *Proceedings of EUSIPCO-94*, volume 1, pages 147–150, Edinburgh, UK, Sep. 1994.

[16] M. Ghanbari, S. De Faria, I.N. Goh, and K.T. Tan. Motion compensation for very low bit-rate video. *Signal Processing: Image Communication*, 7(4-6):567–580, Nov. 1995.

[17] D. Giusto, C. Regazzoni, S. Serpico, and G. Vernazza. A new adaptive approach to picture coding. *Annales des Télécommunications*, 45(9-10):503–518, 1990.

[18] R.C. Gonzalez and R.E. Woods. *Digital Image Processing.* Addison-Wesley, Reading, MA, third edition, 1992.

[19] C. Gu and M. Kunt. Contour simplification and motion compensation for very low bit-rate video coding. In *Proceedings ICIP-94*, volume II, pages 423–427, Austin, Texas, November 1994. IEEE, IEEE Computer Society Press.

[20] C. Gu and M. Kunt. Very low bit-rate video coding using multi-criterion segmentation. In *Proceedings ICIP-94*, volume II, pages 418–422, Austin, Texas, November 1994. IEEE, IEEE Computer Society Press.

[21] V.K. Heer and H.E. Reinfelder. A comparison of reversible methods for data compression. In *Proceedings of Medical Imaging IV*, volume 1233, pages 354–365. SPIE, 1990.

[22] I. Hussain and T.R. Reed. Segmentation-based image compression with enhanced treatment of textured regions. In *Proceedings of the Twenty-Eighth Asilomar Conference on Signals, Systems and Computers*, volume 2, pages 965–969, Pacific Grove, CA, 1994. IEEE Comput. Soc. Press.

[23] J.D. Johnston. A filter family designed for use in quadrature mirror filter banks. In *Proceedings ICASSP*, pages 291–294, Denver, CO, 1980.

[24] M.B. Kim, Y.D. Cho, D.K. Kim, and N.K. Ha. On the compression of medical images with regions of interest (ROIs). In *Visual Communications and Image Processing '95*, volume 2501(1), pages 733–44, Taipei, Taiwan, May 1995. SPIE.

[25] M. Kocher and M. Kunt. A contour-texture approach to picture coding. In *Proceedings ICASSP*, pages 436–440, 1982.

[26] M. Kunt, M. Bénard, and R. Leonardi. Recent results in high compression image coding. *IEEE Trans. Circuits and Systems*, CAS-34(11):1306–1336, Nov. 1987.

[27] M. Kunt, A. Ikonomopoulos, and M. Kocher. Second-generation image-coding techniques. *Proc. IEEE*, 73:549–574, 1985.

[28] O. Kwon and R. Chellapa. Region based subband image coding scheme. In *Proceedings ICIP-94*, volume II, pages 859–863, Austin, Texas, November 1994. IEEE, IEEE Computer Society Press.

[29] F. Lavagetto, F. Cocurullo, and S. Curinga. Frame adaptive segmentation for model-based videophone coding. In *Proceedings ICIP-94*, volume II, pages 414–417, Austin, Texas, November 1994. IEEE, IEEE Computer Society Press.

[30] J.B. Lee, S.D. Kim, and S.Z. Lee. Selective coding method based on motion information. In *Proceedings of EUSIPCO-94*, volume 2, pages 676–679, Edinburgh, UK, Sep. 1994.

[31] D. LeQuang and A. Zaccarin. A new object-oriented approach for video compression at very low bit rate. In F. Gagnon, editor, *Proceedings 1995 Canadian Conference on Electrical and Computer Engineering*, volume 2, pages 823–826. IEEE, Sep. 1995.

[32] W. Li, V. Bhaskaran, and M. Kunt. Very low bit-rate video coding with DFD segmentation. *Signal Processing: Image Communication*, 7(4-6):419–434, Nov. 1995.

[33] F. Moscheni, F. Dufaux, I. Moccagatta, and M. Schutz. A new motion field enhancement technique for video coding. In *Proceedings of EUSIPCO-94*, volume 2, pages 692–695, Edinburgh, UK, Sep. 1994.

[34] Y. Ohtaki, K. Toraichi, T. Horiuchi, and F. Nagasaki. Data compression method of left ventricular cineangiograms for their digital database system. In *IEEE Pacific Rim Conference on Communications, Computers and Signal Processing*, volume 2, pages 602–5, Victoria, BC, Canada, May 1993. IEEE.

[35] K.O. Perlmutter, S.M. Perlmutter, P.C. Cosman, E.A. Riskin, R.A. Olshen, and R.M. Gray. Tree-structured vector quantization with region-based classification. In *Proc. Twenty-sixth Asilomar Conference on Signals, Systems and Computers*, Pacific Grove, CA, Oct. 1992.

[36] K.O. Perlmutter, W. Tchoi, S.M. Perlmutter, and P.C. Cosman. Wavelet/TSVQ image coding with segmentation. In *Proc. Twenty-ninth Asilomar Conference on Signals, Systems and Computers*, Pacific Grove, CA, Nov. 1995.

[37] G. Poggi and R.A. Olshen. Pruned tree-structured vector quantization of medical images with segmentation and improved prediction. *IEEE Trans. Image Processing*, 4(6):734–742, June 1995.

[38] M. Rabbani and P. W. Jones. *Digital Image Compression Techniques*, volume TT7 of *Tutorial Texts in Optical Engineering*. SPIE Optical Engineering Press, Bellingham, WA, 1991.

[39] S. Ranganath and H. Blume. Hierarchical image decomposition and filtering using the S-transform. In *Proceedings of Medical Imaging II*, volume 914, pages 799–814. SPIE, 1988.

[40] T.W. Ryan, L.D. Sanders, and H.D. Fisher. Wavelet-domain texture modeling for image compression. In *Proceedings ICIP-94*, volume II, pages 380–384, Austin, Texas, November 1994. IEEE, IEEE Computer Society Press.

[41] A. Said and W.A. Pearlman. A new fast and efficient image codec based on set partitioning in hierarchical trees. *IEEE Trans. on Circuits and Systems for Video Technology*, to appear.

[42] A. Said and W.A. Pearlman. Reversible image compression via multiresolution representation and predictive coding. In *Proceedings SPIE Symposium on Visual Communications and Image Processing*, volume 2094(2), pages 664–74, Cambridge, MA, Nov 1993.

[43] P. Salembier, L. Torres, F. Meyer, and C. Gu. Region-based video coding using mathematical morphology. *Proceedings of the IEEE*, 83(6):843–857, June 1995.

[44] J. Shapiro. Embedded image coding using zerotrees of wavelet coefficients. *IEEE Transactions on Signal Processing*, 41(12):3445–3462, December 1993.

[45] L. Shen and R.M. Rangayyan. Segmentation-based lossless coding of medical images. In *Visual Communications and Image Processing '95*, volume 2501(2), pages 974–82, Taipei, Taiwan, May 1995. SPIE.

[46] T. Sikora, S. Bauer, and B. Makai. Efficiency of shape-adaptive 2-D transforms for coding of arbitrarily shaped image segments. *IEEE Trans. on Circuits and Systems for Video Technology*, 5(3):254–8, June 1995.

[47] C.C. Sim, W.C. Wong, and K. Ong. Segmented approach for lossless compression of medical images. In *Proceedings of IEEE Singapore International Conference on Networks/International Conference on Information Engineering '93*, volume 2, pages 554–7, Singapore, Sept. 1993. IEEE.

[48] C. Stiller and J. Konrad. Region-adaptive transform based on a stochastic model. In *Proceedings ICIP-95*, volume II, pages 264–7, Washington, D.C., October 1995. IEEE, IEEE Computer Society Press.

[49] C. Swain and T. Chen. Defocus-based image segmentation. In *Proceedings ICASSP-95*, volume 4, pages 2403–6, Detroit, MI, May 1995. IEEE.

[50] S. Takamura and M. Takagi. Lossless image compression with lossy image using adaptive prediction and arithmetic coding. In J.A. Storer and M. Cohn, editors, *Proceedings of the 1994 IEEE Data Compression Conference*, pages 166–174, Snowbird, Utah, 1994. IEEE Computer Society Press.

[51] D. Tzovaras, N. Grammalidis, and M.G. Strintzis. Joint three-dimensional motion/disparity segmentation for object-based stereo image sequence coding. *Optical Engineering*, 35(1):137–144, Jan. 1995.

[52] A. Vlaicu, S. Lungu, N. Crisan, and S. Persa. New compression techniques for storage and transmission of 2-D and 3-D medical images. In *Advanced Image and Video Communications and Storage Technologies*, volume 2451, pages 370–7, Amsterdam, Netherlands, March 1995. SPIE.

[53] H.S. Wong, L. Guan, and H. Hong. Compression of digital mammogram databases using a near-lossless scheme. In *Proceedings ICIP-95*, volume II, pages 21–24, Washington, D.C., October 1995. IEEE, IEEE Computer Society Press.

[54] Y. Yokoyama, Y. Miyamoto, and M. Ohta. Very low bit rate video coding using arbitrarily shaped region-based motion compensation. *IEEE Transactions on Circuits and Systems for Video Technology*, 5(6):500–507, Dec. 1995.

[55] H. Zheng and S.D Blostein. Motion-based object segmentation and estimation using the MDL principle. *IEEE Trans. Image Processing*, 4(9):1223–35, Sep. 1995.

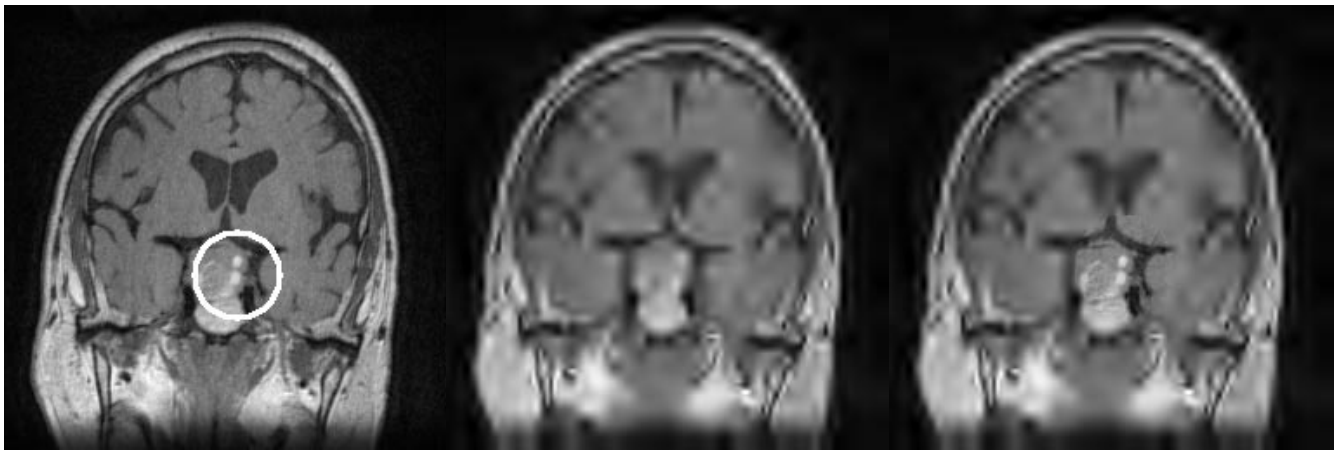

Figure 1: MR brain scan with tumors circled (a), MR brain scan compressed by a factor of 100:1 (b), compressed scan with circled region shown at original accuracy (c).

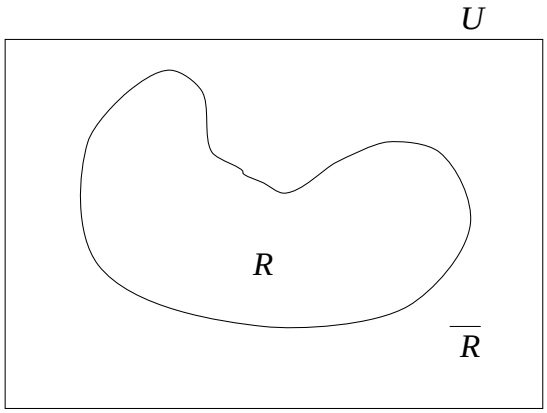

Figure 2: Region R is encoded with method M_1 to quality level Q_1. Region $\bar{R}$ is encoded with method M_2 to quality level Q_2.

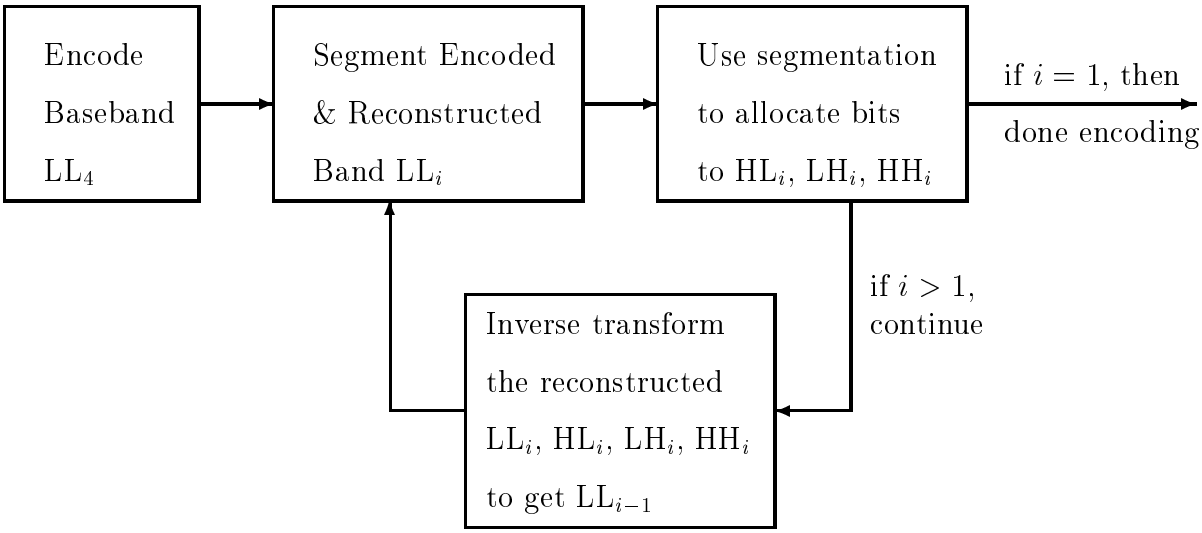

Figure 3: The encoder in [36] achieves different quality levels by recursively segmenting, quantizing based on the segmentation, and inverse transforming.

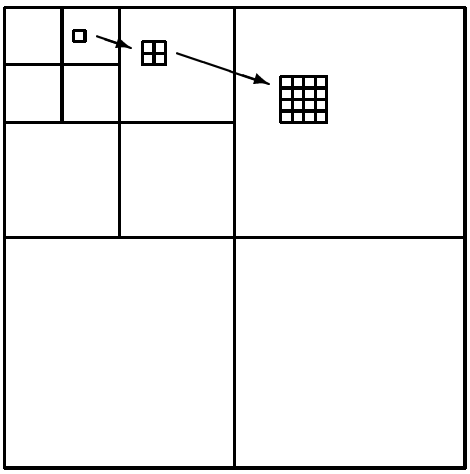

Figure 4: Parent-child relationships in octave-band subbands

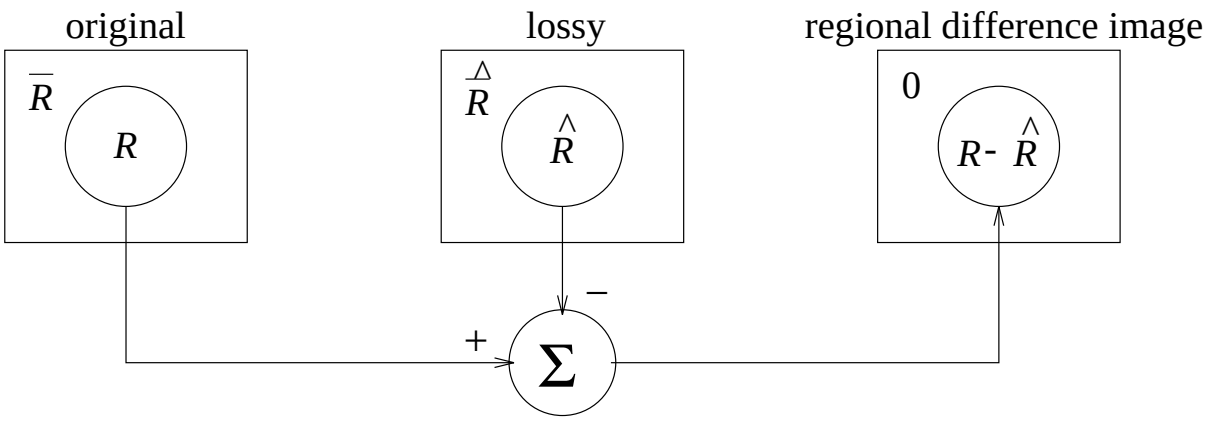

Figure 5: Regional difference image.

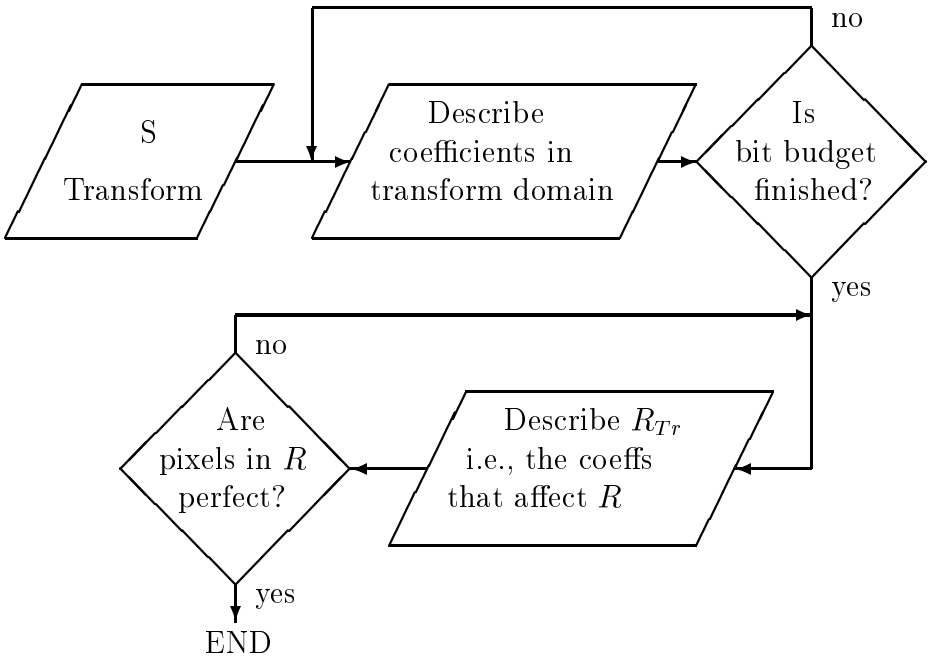

Figure 6: Flow graph of the S-algorithm.

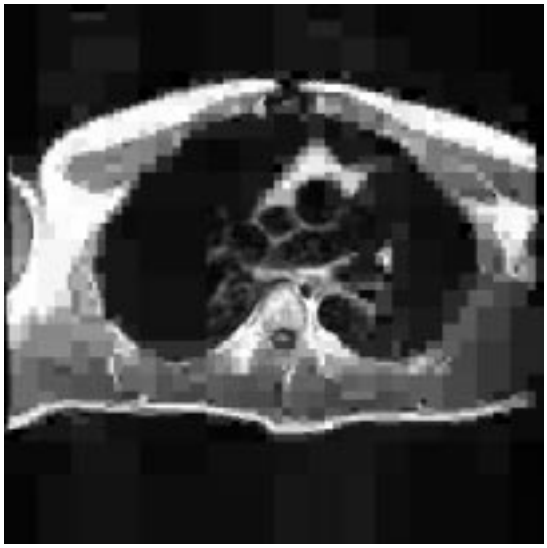

Figure 7: Block artifacts of the S-transform.

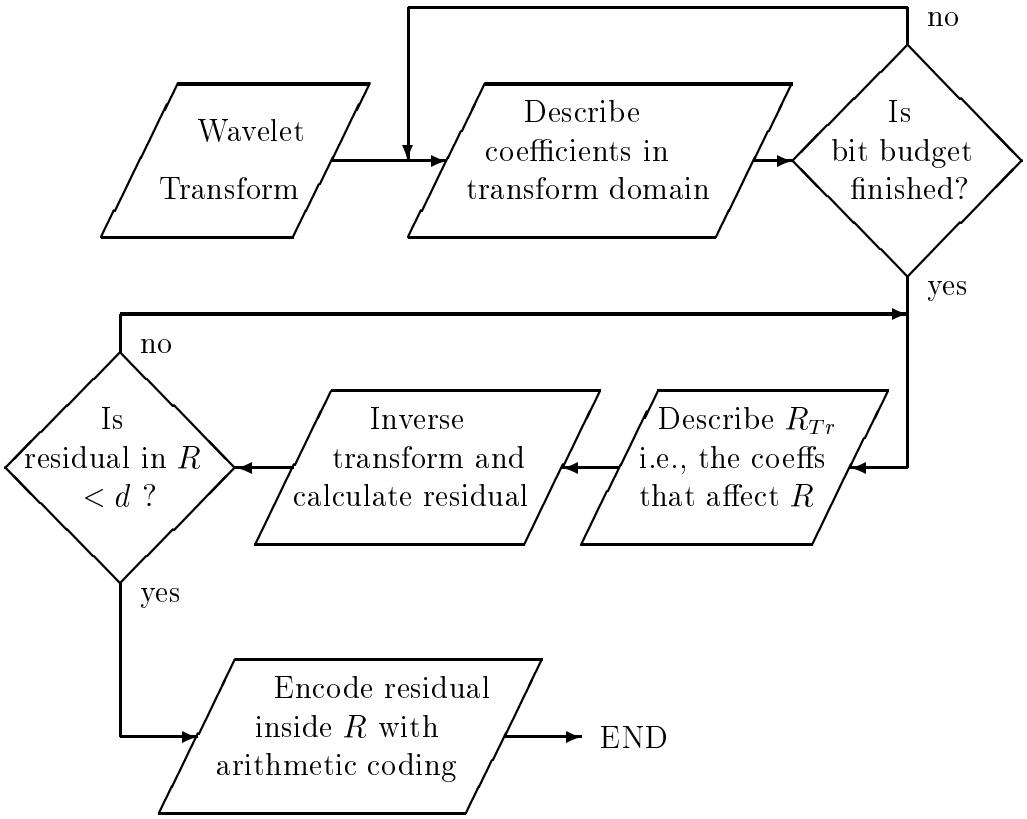

Figure 8: Flow graph of the WA-algorithm.

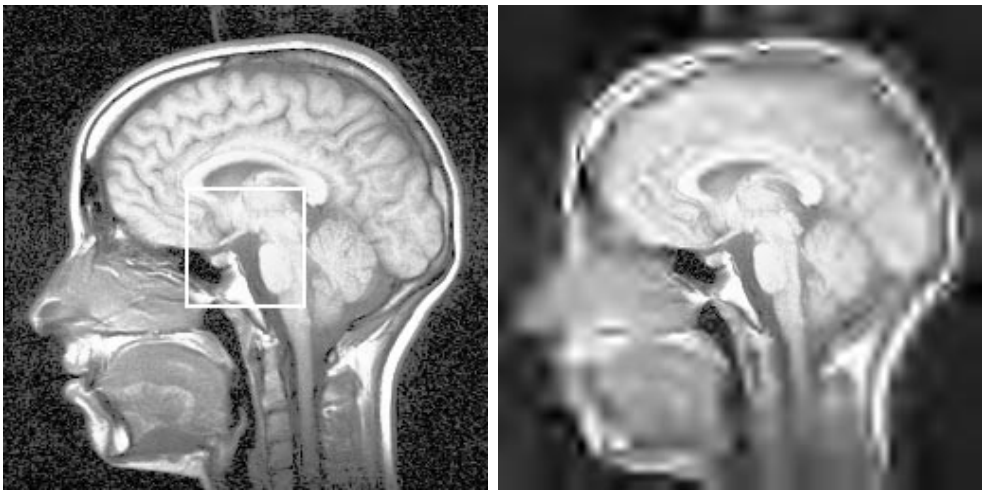

Figure 9: The quality from the ROI region (left) spreads out to the surrounding pixels (right). A background PSNR as low as 20 dB is used in this example to clearly show the effect.

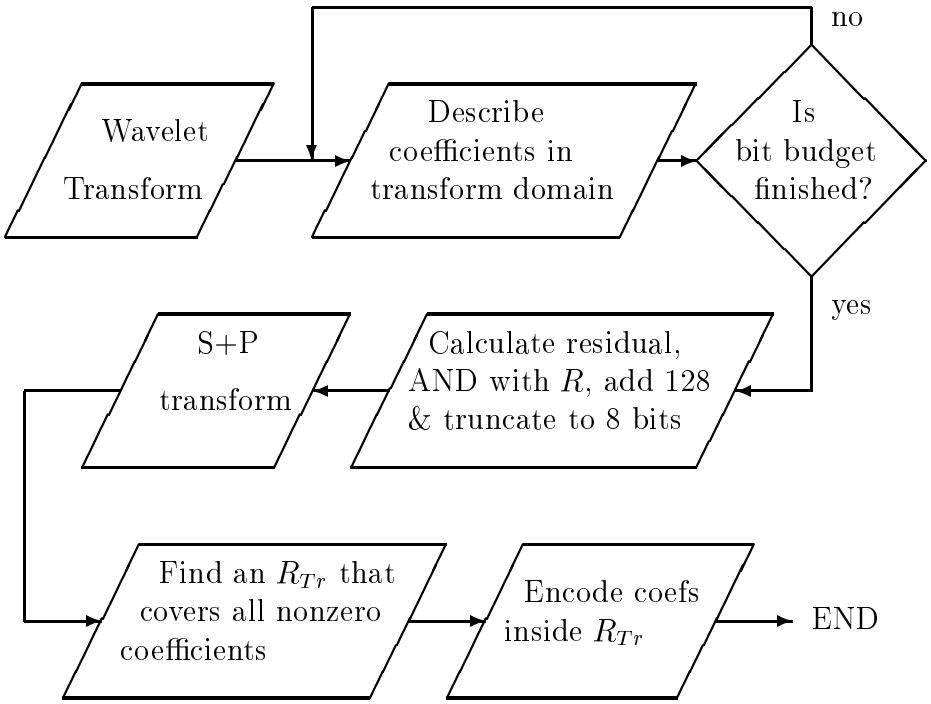

Figure 10: Flow graph of the WSP-algorithm.

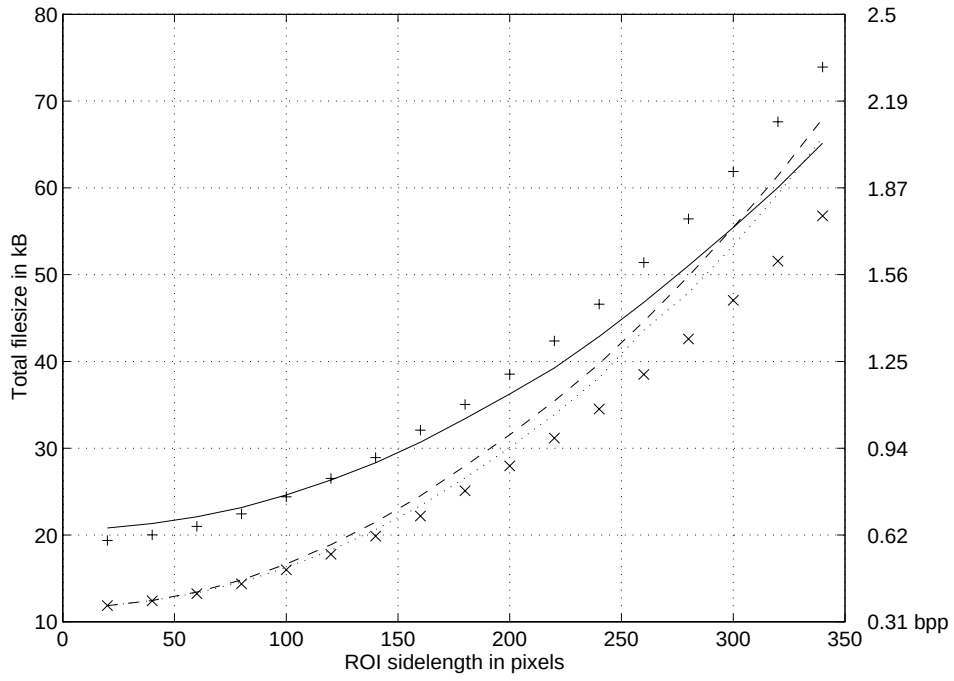

Figure 11: Comparison of all methods for a CT scan: DCT/LZ (+), S-algorithm (solid), WA-algorithm (dots), W/LZ (dashes), WS+P algorithm (x).

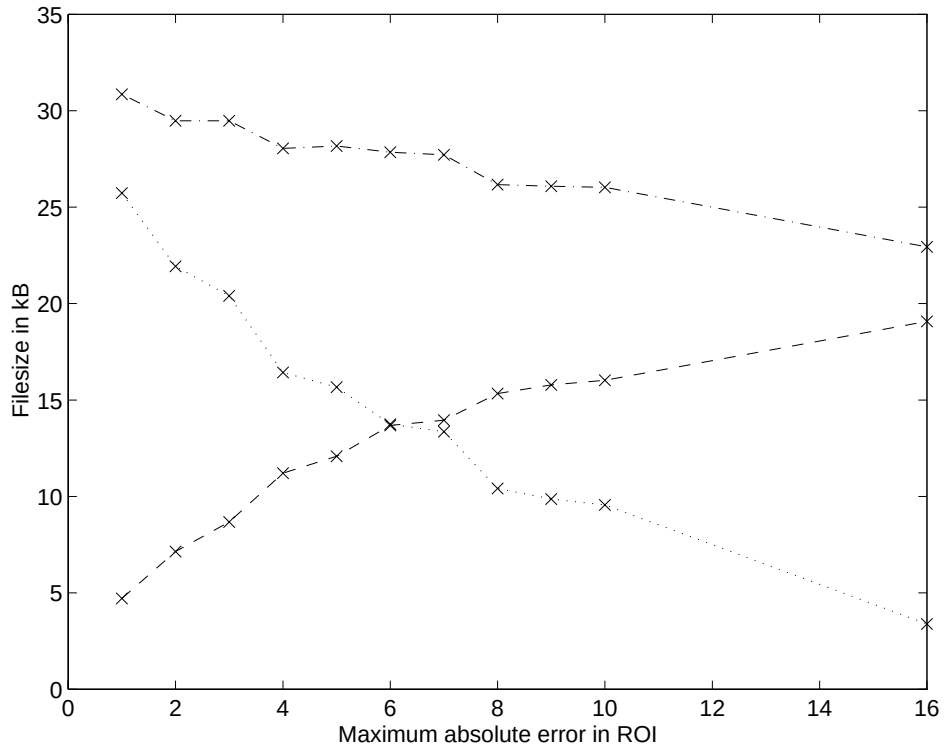

Figure 12: File size in kbytes vs. maximum absolute error remaining in the ROI for arithmetic encoding. Dotted line: bytes used by the wavelet zerotree coder. Dashed line: bytes used by the arithmetic coder. Dot-dash line: total number of bytes.

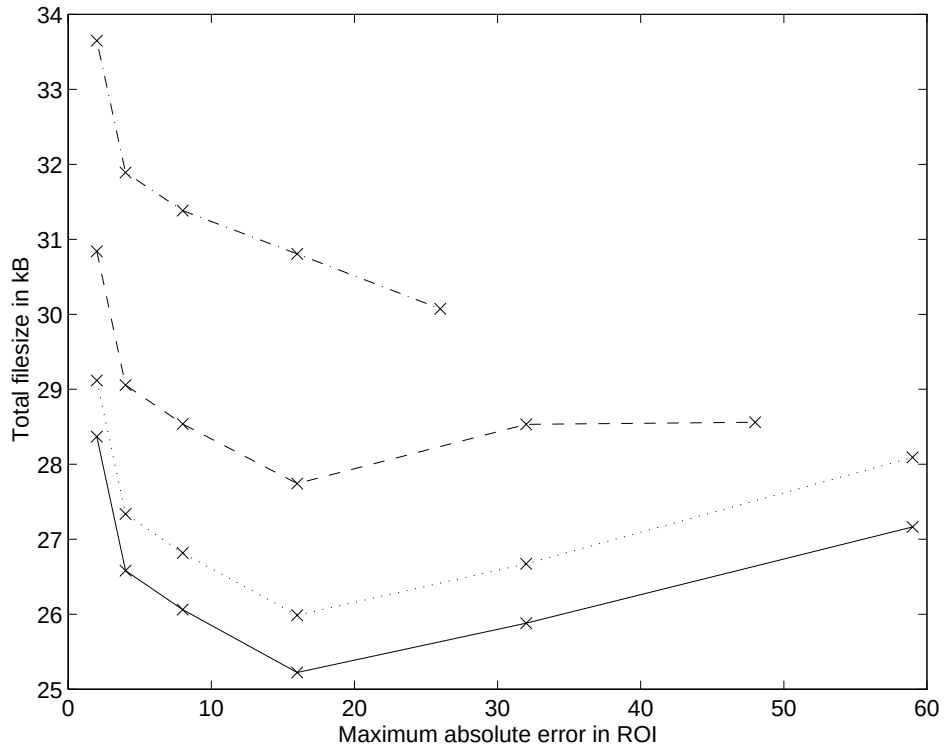

Figure 13: File size in kbytes vs. maximum absolute error remaining in the ROI for arithmetic encoding. The ROI size is fixed. The background PSNR is varied: 28 dB (solid), 32 dB (dotted), 36 dB (dashed) and 40 dB (dash-dot).

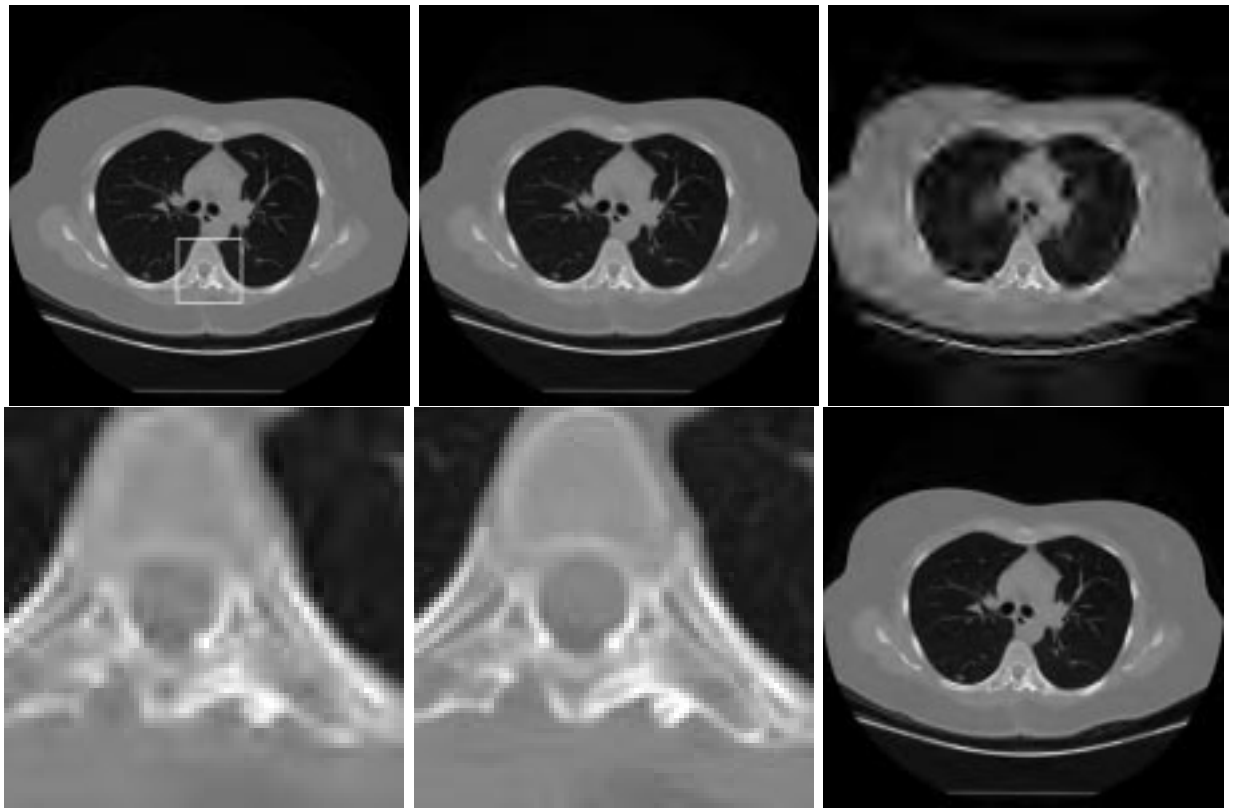

Figure 14: Top row from left: (a) Original image with circled ROI, (b) Lossy image, size 3953 bytes, (c) Lossless inside ROI, 3953 bytes, Bottom row from left: (d) Zoom on lossy ROI, (e) Zoom on original ROI, (f) Lossless inside ROI, 7189 bytes.

List of Figures